

Searching Axion-like Dark Matter by Amplifying Weak Magnetic Field with Quantum Zeno effect

Jing Dong,^{1,2,3,4} W. T. He,⁵ S.-D. Zou,¹ D. L. Zhou,^{2,3} and Qing Ai^{1,4,*}

¹*School of Physics and Astronomy, Applied Optics Beijing Area Major Laboratory, Beijing Normal University, Beijing 100875, China*

²*Institute of Physics, Chinese Academy of Sciences, Beijing 100190, China*

³*University of Chinese Academy of Sciences, Beijing 100049, China*

⁴*Key Laboratory of Multiscale Spin Physics, Ministry of Education, Beijing Normal University, Beijing, China*

⁵*Quantum Dynamics Unit, Okinawa Institute of Science and Technology, Tancha 1919-1, Okinawa 904-0495, Japan*

(Dated: February 20, 2025)

The enhancement of weak signals and the detection of hypothetical particles, facilitated by quantum amplification, are crucial for advancing fundamental physics and its practical applications. Recently, it was experimentally observed that magnetic field can be amplified by using nuclear spins under Markovian noise, [H. Su, *et al.*, *Phys. Rev. Lett.* **133**, 191801 (2024)]. Here, we theoretically propose amplifying the magnetic-field signal by using nuclear spins by the quantum Zeno effect (QZE). Under identical conditions, we demonstrate that compared to the Markovian case the amplification of the weak magnetic field can be enhanced by a factor about $e^{1/2}$ under a Gaussian noise. Moreover, through numerical simulations we determine the optimal experimental parameters for amplification conditions. This work shows that the combination of the QZE and spin amplification effectively enhances the amplification of the weak magnetic field. Our findings may provide valuable guidance for the design of experiments on establishing new constraints of dark matter and exotic interactions in the near future.

I. INTRODUCTION

According to astrophysical observations, roughly five sixths of the matter in the universe remains dark [1]. However, direct detection of its interactions with particles and fields of the standard model remains elusive [2]. There are a variety of particle candidates for dark matter, such as quantum chromodynamics axion and axion-like particles (ALPs) [3], new Z' bosons [4], new spin-1 bosons [5] and dark photons [6, 7]. Axions are prominent dark-matter and dark-energy candidates, which are introduced as a compelling solution to the strong-CP problem beyond the standard model. However, it is insufficient to search for ALPs by traditional particle-physics techniques with light quanta such as the Large Hadron Collider [8, 9]. Therefore, experimental searches for axion-like dark matter are based on their non-gravitational interactions with particles and fields of the standard model [8–14].

As known to all, quantum amplification plays an important role in quantum metrology and finds applications in the measurements of weak field and force [15–18], and optical amplification [19] to search for new physics beyond the standard model [10]. Besides, the magnetic-field amplification finds applications in a wide range of searching axion-nucleon interactions, such as ALPs and axion bursts from astrophysical events [20, 21]. Under the state-of-art experiments, the sensitivity has exceeded astrophysical limits [22] by several orders of magnitude. We note that both electron

and nuclear spins have shown great potential for realizing signal amplification. For example, the overlapping spin ensemble, e.g. ^{129}Xe - ^{87}Rb , is used in self-compensating comagnetometers [23–25]. Recently, the magnetic-field amplification using ^{129}Xe noble gas overlapping with spin-polarized ^{87}Rb atomic gas is demonstrated, which has achieved a significant improvement in amplification of weak-field measurements under the Markovian noise, i.e., a constant spin relaxation rate [26].

On the other hand, the QZE describes the phenomenon that a quantum system's dynamic evolution drastically slows down when measured frequently enough [27–31]. The QZE plays a pivotal role in various domains of quantum science. One of the applications of the QZE is the quantum measurements, which can suppress the detrimental effects of decoherence [32, 33]. By performing frequent error-correction measurements, the QZE helps stabilize the quantum state of qubits, thereby prolonging their coherence time and enhancing the reliability of quantum computations. Both theoretically and experimentally, it has been demonstrated that the QZE can enhance the quantum metrology by using the maximum-entangled states [34–36]. So far, the QZE has been experimentally observed in a number of physical systems such as trapped ions [37, 38], ultracold atoms [39–41], molecules [42], Bose-Einstein condensates [43], nitrogen-vacancy centers [44] and superconducting quantum circuits [45–48].

To achieve the more significant amplification of external magnetic fields, in this paper, we propose a magnetic-field amplification using noble gas overlapping with spin-polarized alkali-metal gas by the QZE, which can achieve an improvement in the amplification of weak-field measurements as compared to the Markovian

* aiqing@bnu.edu.cn

case. In weak magnetic fields, we obtain the analytical solution to the dynamics of ^{129}Xe spins and amplification function, which present an enhancement of $e^{1/2}$ compared to Markovian case. In the case of strong magnetic fields, we further examine the response of the ^{129}Xe spins by numerical simulations under various conditions. Then, we provide the optimal measurement parameters for the practical experiments, i.e., the detuning between the Larmor frequency and the frequency of magnetic field, the decoherence time, and the magnitude of the magnetic field. We anticipate that the present amplification technique could stimulate possible applications in applied and fundamental physics.

The rest of the paper is organized as follows. The model is set up and the response of polarized ^{129}Xe spins to a transverse oscillating magnetic field is derived in Sec. II. Then, the response of polarized ^{129}Xe spins in the case of weak magnetic fields is investigated in Sec. III. In Sec. IV, the transverse polarization of the polarized ^{129}Xe spins is studied and the optimal amplification is explored in the case of strong magnetic fields. A summary is concluded in Sec. V.

II. MODEL

According to Ref. [49], there are two cells containing nuclear spins, i.e., the source and the sensor cells. In order to polarize the Rb spins and thus the ^{129}Xe nuclear spins, a static magnetic field with strength B_0 is applied along z -axis. Due to the axion-mediated interaction between polarized neutrons, the ^{129}Xe nuclear spins are also subject to a time-dependent transverse magnetic field. As a result, the ^{129}Xe nuclear spin in a magnetic field is described by the following Hamiltonian

$$\hat{H} = -\gamma_n \mathbf{B}(t) \cdot \hat{\mathbf{I}}, \quad (1)$$

where $\mathbf{B}(t) = B_0 \hat{z} + B_{ac} \cos(2\pi\nu t) \hat{y}$ is the total field experienced by ^{129}Xe nuclear spins with ν being the Larmor frequency of the nuclear spins in the source cell, $\gamma_n = 2\pi \times 11.78 \text{ Hz}/\mu\text{T}$ [26] and $\hat{\mathbf{I}} = (\hat{I}_x, \hat{I}_y, \hat{I}_z)$ are the gyromagnetic ratio and the angular momentum operators of ^{129}Xe , respectively. Thus, the Larmor frequency of ^{129}Xe is

$$\nu_0 = \frac{\gamma_n B_0}{2\pi}, \quad (2)$$

where γ_n is the gyromagnetic ratio of ^{129}Xe . The spin Hamiltonian with the total field reads explicitly

$$\hat{H} = -\gamma_n B_0 \hat{I}_z - \gamma_n B_{ac} \cos(2\pi\nu t) \hat{I}_y. \quad (3)$$

According to the Heisenberg equation of motion, we can obtain the dynamical equation for the nuclear spin

angular momentum as

$$\frac{d\hat{I}_x}{dt} = \gamma_n B_0 \hat{I}_y - \gamma_n B_{ac} \cos(2\pi\nu t) \hat{I}_z, \quad (4)$$

$$\frac{d\hat{I}_y}{dt} = -\gamma_n B_0 \hat{I}_x, \quad (5)$$

$$\frac{d\hat{I}_z}{dt} = \gamma_n B_{ac} \cos(2\pi\nu t) \hat{I}_x. \quad (6)$$

The polarization of ^{129}Xe atoms can be defined as

$$\mathbf{P} = \frac{\langle \hat{\mathbf{I}} \rangle}{v_0}, \quad (7)$$

where v_0^{-1} is the atomic number density. The dynamics of the three polarization components can be described by the Bloch equations as [50]

$$\frac{dP_x}{dt} = \gamma_n B_0 P_y - \gamma_n B_{ac} \cos(2\pi\nu t) P_z, \quad (8)$$

$$\frac{dP_y}{dt} = -\gamma_n B_0 P_x, \quad (9)$$

$$\frac{dP_z}{dt} = \gamma_n B_{ac} \cos(2\pi\nu t) P_x. \quad (10)$$

Generally speaking, any quantum system inevitably suffers from the interaction with its environment. On account of a Markovian noise, the dynamics of ^{129}Xe spins can be described with the Bloch equations

$$\frac{dP_x}{dt} = \gamma_n B_0 P_y - \gamma_n B_{ac} \cos(2\pi\nu t) P_z - \frac{1}{T_2} P_x, \quad (11)$$

$$\frac{dP_y}{dt} = -\gamma_n B_0 P_x - \frac{1}{T_2} P_y, \quad (12)$$

$$\frac{dP_z}{dt} = \gamma_n B_{ac} \cos(2\pi\nu t) P_x - \frac{1}{T_1} P_z, \quad (13)$$

where T_1 (T_2) is the longitudinal (transverse) relaxation time of ^{129}Xe spin. We consider the response of polarized ^{129}Xe spins to a transverse oscillating magnetic field. Considering a Gaussian noise, the dynamics of ^{129}Xe spins can be described by the Bloch equation as [51]

$$\frac{dP_x}{dt} = \gamma_n B_0 P_y - \gamma_n B_{ac} \cos(2\pi\nu t) P_z - \frac{t}{T_2^2} P_x, \quad (14)$$

$$\frac{dP_y}{dt} = -\gamma_n B_0 P_x - \frac{t}{T_2^2} P_y, \quad (15)$$

$$\frac{dP_z}{dt} = \gamma_n B_{ac} \cos(2\pi\nu t) P_x - \frac{t}{T_1^2} P_z. \quad (16)$$

To analyze the system more conveniently, we transform it to the rotating frame defined by

$$\hat{U} = e^{i2\pi\nu t \hat{I}_z}. \quad (17)$$

In the rotating frame, the effective Hamiltonian

$$\hat{H} = \hat{U}^\dagger \hat{H} \hat{U} - i\hat{U}^\dagger \frac{d}{dt} \hat{U} \quad (18)$$

can be simplified as

$$\hat{H} \approx \Delta \hat{I}_z - \frac{1}{2} \gamma_n B_{ac} \hat{I}_y, \quad (19)$$

where $\Delta = 2\pi(\nu - \nu_0)$ is the detuning, and we have dropped the fast-oscillating terms by the rotating-wave approximation [30, 51]. Thus, the Bloch equations of ^{129}Xe spins in the rotating frame read

$$\dot{\tilde{P}}_x = \frac{\gamma_n B_{ac}}{2} \tilde{P}_z + \Delta \tilde{P}_y - \frac{t}{T_2} \tilde{P}_x, \quad (20)$$

$$\dot{\tilde{P}}_y = -\Delta \tilde{P}_x - \frac{t}{T_2} \tilde{P}_y, \quad (21)$$

$$\dot{\tilde{P}}_z = -\frac{\gamma_n B_{ac}}{2} \tilde{P}_x - \frac{t}{T_1} \tilde{P}_z, \quad (22)$$

where \tilde{P}_α ($\alpha = x, y, z$) are the polarization of ^{129}Xe spins in the rotating frame. According to Eq. (2), we can define the effective magnetic field in the rotating frame as $\tilde{\mathbf{B}} = (B_{ac}/2)\hat{y} - (\Delta/\gamma_n)\hat{z}$.

When the Rb pump light is off, the effective magnetic-field gradient induced by the Rb polarization is greatly suppressed, resulting in T_2 being close to T_1 [49]. As a result, we assume $T_2 \approx T_1 = T$ and thus we have

$$\dot{\tilde{P}}_x = \frac{\gamma_n B_{ac}}{2} \tilde{P}_z + \Delta \tilde{P}_y - \frac{t}{T} \tilde{P}_x, \quad (23)$$

$$\dot{\tilde{P}}_y = -\Delta \tilde{P}_x - \frac{t}{T} \tilde{P}_y, \quad (24)$$

$$\dot{\tilde{P}}_z = -\frac{\gamma_n B_{ac}}{2} \tilde{P}_x - \frac{t}{T} \tilde{P}_z. \quad (25)$$

III. LINEAR RESPONSE

In practical applications, precise measurement of weak magnetic fields is often of great interest, such as those associated with precision medicine, deep-sea exploration and cardiac activity, etc [26]. When B_{ac} is weak enough, we can ignore the first term in Eq. (25). In this case, the time evolution of \tilde{P}_z is decoupled with \tilde{P}_x , \tilde{P}_y and B_{ac} . And \tilde{P}_x exhibits a linear dependence on B_{ac} . Under the weak-field approximation, Eqs. (23)-(25) can be simplified as

$$\dot{\tilde{P}}_x = \frac{\gamma_n B_{ac}}{2} \tilde{P}_z + \Delta \tilde{P}_y - \frac{t}{T} \tilde{P}_x, \quad (26)$$

$$\dot{\tilde{P}}_y = -\Delta \tilde{P}_x - \frac{t}{T} \tilde{P}_y, \quad (27)$$

$$\dot{\tilde{P}}_z = -\frac{t}{T} \tilde{P}_z. \quad (28)$$

When the polarization is initially along z -axis, i.e., $\mathbf{P}(t=0) = (0, 0, P_0)$, the solutions to the above equations can

be expressed as follows

$$\tilde{P}_x = \frac{P_0 B_{ac} \gamma_n}{2\Delta} e^{-\frac{t^2}{2T^2}} \sin(\Delta t), \quad (29)$$

$$\tilde{P}_y = \frac{P_0 B_{ac} \gamma_n}{2\Delta} e^{-\frac{t^2}{2T^2}} [\cos(\Delta t) - 1], \quad (30)$$

$$\tilde{P}_z = P_0 e^{-\frac{t^2}{2T^2}}. \quad (31)$$

Since the relation between the polarization in the rotating frame and the laboratory frame is

$$P_x(t) = \tilde{P}_x(t) \cos(\omega t) - \tilde{P}_y(t) \sin(\omega t), \quad (32)$$

$$P_y(t) = \tilde{P}_x(t) \sin(\omega t) + \tilde{P}_y(t) \cos(\omega t), \quad (33)$$

$$P_z(t) = \tilde{P}_z(t), \quad (34)$$

we can obtain the polarization in the laboratory frame as

$$P_x = \frac{P_0 B_{ac} \gamma_n}{2\Delta} e^{-\frac{t^2}{2T^2}} [\sin(\Delta t - \omega t) + \sin(\omega t)], \quad (35)$$

$$P_y = \frac{P_0 B_{ac} \gamma_n}{2\Delta} e^{-\frac{t^2}{2T^2}} [\cos(\Delta t - \omega t) - \cos(\omega t)], \quad (36)$$

$$P_z = P_0 e^{-\frac{t^2}{2T^2}}. \quad (37)$$

Thus, the magnitude of the transverse polarization can be expressed as

$$P_\perp = \frac{P_0 B_{ac} \gamma_n}{\Delta} e^{-\frac{t^2}{2T^2}} \sin\left(\frac{\Delta t}{2}\right). \quad (38)$$

According to $B_{\text{eff}} = 8\pi\kappa_0 M_0 P_\perp / 3$, where $\kappa_0 = 540$ denotes the Fermi-contact enhancement factor between ^{129}Xe and ^{87}Rb [26, 52], the amplitude of the transverse effective field is

$$B_{\text{eff}} = \frac{8\pi}{3} \kappa_0 M_0 \frac{P_0 B_{ac} \gamma_n}{\Delta} e^{-\frac{t^2}{2T^2}} \sin\left(\frac{\Delta t}{2}\right). \quad (39)$$

And thus the transverse field is amplified by a factor

$$\Pi \equiv \frac{|B_{\text{eff}}|}{|B_{ac}|} = \frac{2\lambda M_n \gamma_n}{\Delta} \sin\left(\frac{\Delta t}{2}\right) e^{-\frac{t^2}{2T^2}}, \quad (40)$$

where $M_n = M_0 P_0$ is the nuclear magnetization of ^{129}Xe , $\lambda = 4\pi\kappa_0/3$. The optimal time t_{opt} can be obtained by calculating $\partial\Pi/\partial t|_{t=t_{\text{opt}}} = 0$, and thus yields $\tan(\Delta t_{\text{opt}}/2) = \Delta T^2/2t_{\text{opt}}$. Now we expand $\tan(\Delta t_{\text{opt}}/2)$ to the third order of Δt_{opt} and obtain the following expression $(\Delta t_{\text{opt}}/2) + (\Delta t_{\text{opt}}/2)^3/3 = \Delta T^2/2t_{\text{opt}}$. The time required to reach the maximum transverse polarization is determined by

$$t_{\text{opt}} = \sqrt{\frac{6}{\Delta^2} \left(-1 + \sqrt{1 + \frac{1}{3} \Delta^2 T^2} \right)}. \quad (41)$$

Again by Taylor expansion, we could obtain

$$t_{\text{opt}} \simeq T \left(1 - \frac{\Delta^2 T^2}{24} \right). \quad (42)$$

Based on this finding, it is shown that the optimal time becomes longer as T increases and Δ decreases, which will be discussed in detail in the next section.

When the oscillation frequency of the external magnetic field matches the ^{129}Xe Larmor frequency, i.e., $\Delta = 0$, the time required to reach the maximum transverse polarization is $t_{\text{opt}} = T$. It should be noted that the optimal time should be smaller than T in the non-resonance case, i.e., $\Delta \neq 0$. The optimal amplification factors for the Markovian and QZE cases are $\Pi = 2\lambda M_n \gamma_n T e^{-1}$ [26] and $\Pi = 2\lambda M_n \gamma_n T e^{-1/2}$, respectively. Therefore, the QZE could enhance the amplification of the weak magnetic field by a factor \sqrt{e} .

IV. NONLINEAR RESPONSE

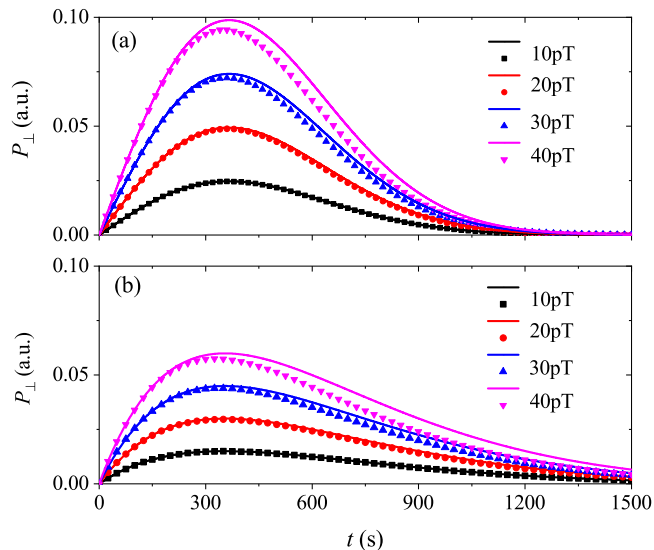


FIG. 1. Time evolution of the transverse polarization P_{\perp} vs B_{ac} for (a) the Gaussian and (b) the Markovian noise, respectively. Solid lines represent the profiles under the linear-response approximation while symbols represent the profiles by the numerically-exact solution. The parameters $T = 380$ s and $\Delta = 2.5$ mHz are used.

In the following, we will obtain the response of the ^{129}Xe spins without the weak-field approximation but by solving Eqs. (23)-(25) numerically. Figure 1 shows P_{\perp} against time in the QZE and Markovian case [26], respectively. In order to verify the validity of the weak-field approximation, we compare the linear response with the nonlinear response under different amplitudes of the magnetic field. The approximated and the exact profiles almost overlap with each other when the measured field is 10 pT. However, as the magnetic field increases, their difference becomes larger and larger, which suggests that the approximation works well in the case of weak fields. Most importantly, it is clearly observed that the response in the former case is significantly larger than that in the

latter, indicating that the magnetic field can be amplified more effectively by the QZE.

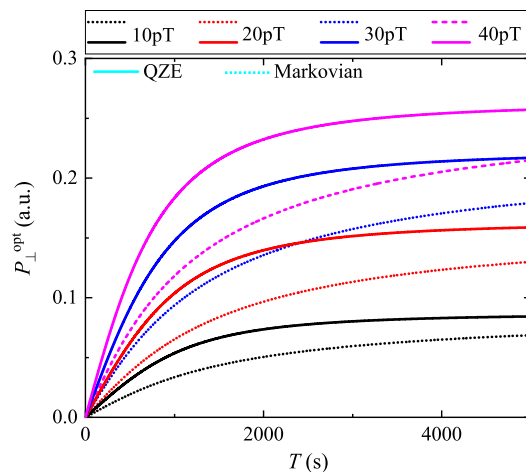


FIG. 2. The optimal transverse polarization P_{\perp}^{opt} as a function of coherence time T for different values of B_{ac} is presented for both Markovian dynamics (dotted lines) and the QZE (solid lines), respectively. The other parameters are the same as those used in Fig. 1.

Figure 2 compares the optimal response P_{\perp}^{opt} in the Markovian case and QZE regime over a wide range of coherence times. It is shown that the optimal responses in both cases exhibit the same trend, gradually increasing with T . Furthermore, the response increases with the magnitude of the magnetic field for a given coherence time T . Interestingly, it is evident that the responses in the QZE consistently exceed those in the Markovian case.

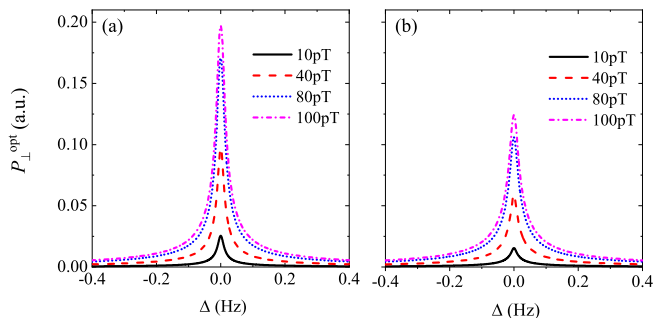


FIG. 3. The optimal transverse polarization P_{\perp}^{opt} in (a) the QZE and (b) the Markovian cases as a function of detuning Δ for different B_{ac} s. The other parameters are the same as those used in Fig. 1.

In order to evaluate the effect of the detuning Δ on the amplification of the magnetic field, as shown in Fig. 3, we compare the optimal responses under the QZE with those in the Markovian case for different B_{ac} s by solving Eqs. (23)-(25) numerically. As illustrated in Fig. 3(a), the optimal response decreases monotonically with increasing detuning for a fixed value of B_{ac} . Therefore, in order

to achieve a larger amplification of the weak magnetic field, the resonance between the driving field and Larmor frequency is required. Furthermore, the optimal response shows a gradual increase as the magnetic field strength is enhanced for a constant detuning. Since we employ the QZE to amplify the weak magnetic field, we further investigate the optimal responses in the Markovian noise in Fig. 3(b). For all B_{ac} s, the optimal response is always smaller than the counterparts in the QZE.

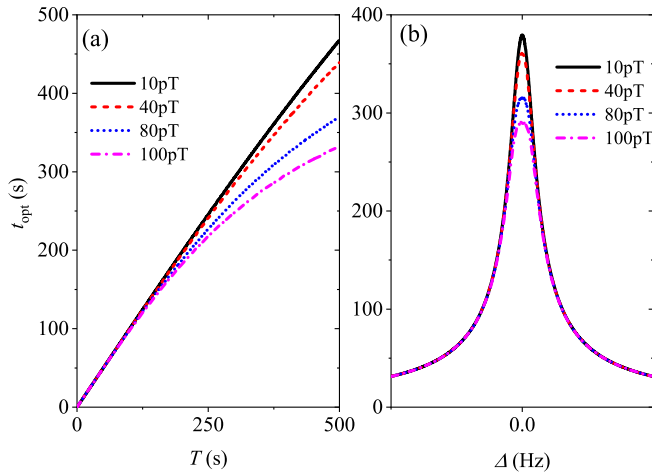


FIG. 4. Dependence of the optimal time t_{opt} on (a) the relaxation time T with $\Delta = 2.5$ mHz and (b) the detuning Δ with $T = 380$ s for the QZE in different B_{ac} s.

In Fig. 4, we present the optimal time t_{opt} to perform the measurement as a function of the relaxation time T and detuning Δ for the QZE, respectively. It is demonstrated that t_{opt} is proportional to T for $B_{ac} = 10$ pT, which is consistent with Eq. (42). However, as B_{ac} increases, the time required to achieve the optimal response decreases for a given T . On the other hand, when talking about the dependence of the optimal measurement time on Δ , it turns out to be much complicated. It requires the longest time to achieve the optimal response for the resonance case, while t_{opt} decreases as the detuning is enlarged, which is predicted by Eq. (42). Notably, for different magnetic fields, all curves coincide with each other in the large-detuning limit. These findings suggest that maximizing the relaxation time while minimizing the detuning is crucial for expediting the amplification of the weak magnetic field. Thus, careful control of these parameters is essential to enhance the efficiency and precision of the measurement process.

Since in Fig. 3(a), the optimal responses increase as the magnetic field is enlarged, it may be quite natural to ask whether there exists a bound for the optimal response. As depicted in Fig. 5, we explore the optimal response for different sets of (B_{ac}, Δ) . When the system is at resonance, the optimal response will quickly be saturated as the magnetic field is enlarged. As the detuning increases, the smallest magnetic field to saturate optimal

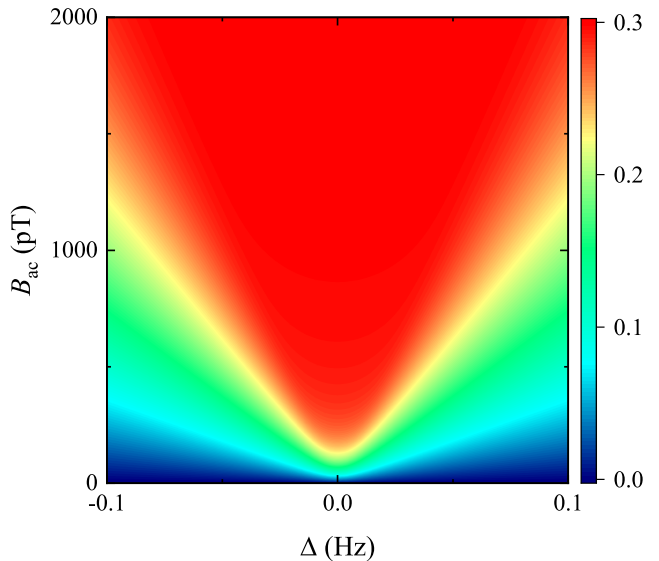


FIG. 5. Phase diagram of the optimal response P_{\perp}^{opt} vs B_{ac} and Δ for $T = 380$ s.

response becomes larger and larger.

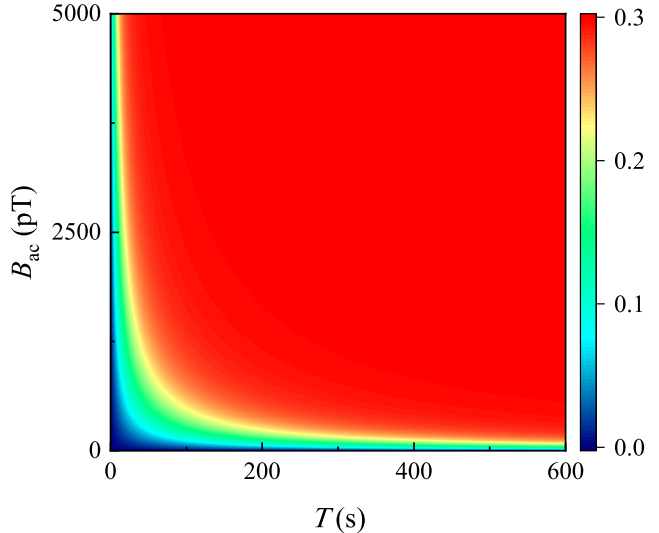


FIG. 6. Phase diagram of the optimal response P_{\perp}^{opt} vs B_{ac} and T for $\Delta = 2.5$ mHz.

To gain further insight into the effects of the amplitude of the oscillating field B_{ac} and the relaxation time T on the optimal response P_{\perp}^{opt} , we focus on the near-resonance case and present the phase diagram of the optimal response for a large range of T and B_{ac} in Fig. 6. It is shown that the optimal response can be achieved across the majority of the parameter space (B_{ac}, T) , which provides convenience for measuring magnetic fields of various amplitudes. However, it should be pointed out that the relaxation time T should be sufficiently large, e.g. $T > 60$ s, in order to attain the maximum optimal response larger than 0.28.

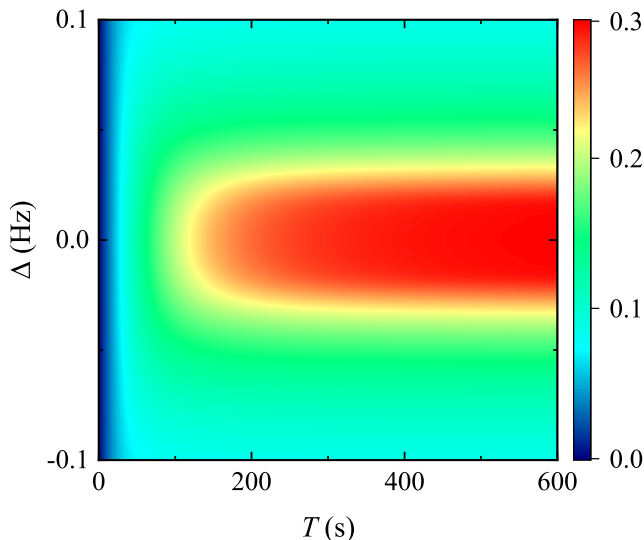


FIG. 7. Phase diagram of the optimal response P_{\perp}^{opt} vs Δ and T for $B_{\text{ac}} = 400$ pT. The other parameters are the same as those in Fig. 1.

In Fig. 7, we explore the optimal response in the parameter space (Δ, T) for $B_{\text{ac}} = 400$ pT. The results indicate that the optimal response is confined to a narrow parameter region, characterized by a large relaxation time T and a small detuning Δ , as depicted by the red region.

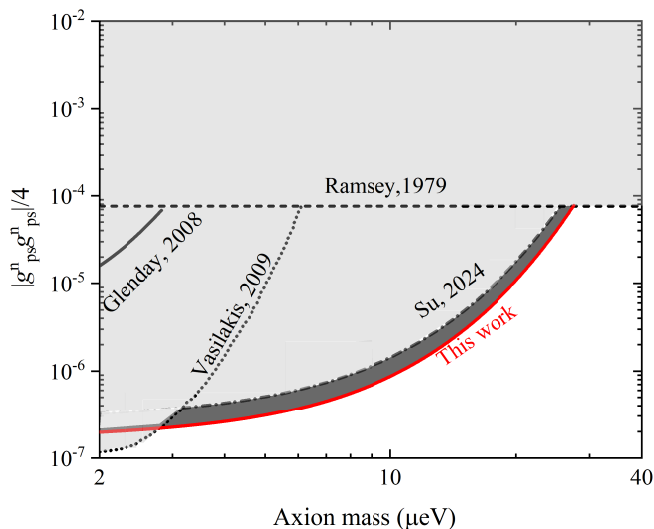


FIG. 8. Constraints to the coupling-constants product $|g_{ps}^n g_{ps}^n|/4$ within the axion window. The black curves represent the experimental limits on the neutron-neutron coupling from the previous experiments of Ramsey [53], Glenday *et al.* [54], Vasilakis *et al.* [25] and Su *et al.* [49] as a function of the axion mass. The red line represents the new constraints on axions or ALPs obtained from our theory, which establishes an improved bound by a factor about $e^{1/2}$ due to the QZE.

According to Refs. [55–57], the interaction between the polarized neutrons is

$$V_{\text{ps-ps}} = \frac{g_{ps}^n g_{ps}^n}{16\pi m_n^2} \left[\hat{\sigma}_{\text{so}} \cdot \hat{\sigma}_{\text{se}} \left(\frac{m_a}{r^2} + \frac{1}{r^3} \right) - (\hat{\sigma}_{\text{so}} \cdot \hat{r})(\hat{\sigma}_{\text{se}} \cdot \hat{r}) \left(\frac{m_a^2}{r} + \frac{3m_a}{r^2} + \frac{3}{r^3} \right) \right], \quad (43)$$

where $\hbar = c = 1$, g_{ps}^n is the pseudoscalar coupling constant of the neutron, m_n (m_a) is the mass of the neutron (axion), $\hat{\sigma}_{\text{so}}$ ($\hat{\sigma}_{\text{se}}$) is the spin operator in the source (sensor) cell, $\vec{r} = r\hat{r}$ is the distance vector between two interacting neutrons. $B_{\text{ac}} \cos(2\pi\nu t)\hat{\sigma}_{\text{so}} = -V_{\text{ps-ps}}/\nu\chi_e$ is the pseudomagnetic field experienced by the nuclear spins in the sensor cell, where ν is the Larmor frequency of the nuclear spin in the sensor cell. Following the same procedure in Ref. [49], we can effectively estimate $|g_{ps}^n g_{ps}^n|/4$. Figure 8 shows the obtained constraints on $|g_{ps}^n g_{ps}^n|/4$ set by this work together with the limits from the previous experimental searches [25, 49, 53, 54]. The excluded values of the coupling-constants product of the previous results are presented as the light-gray areas and the result of this work is presented as the dark-gray area. The first constraint of exotic spin-spin interactions was derived by Ramsey [53] and presented as the black dashed line. The black solid and dotted lines respectively represents the constraints on $|g_{ps}^n g_{ps}^n|/4$ placed by the maser [54] and the comagnetometer [25] experiments. Based on the recent work [49], we set the most stringent constraint on $|g_{ps}^n g_{ps}^n|/4$ by utilizing the QZE from a theoretical perspective and presented as the red solid line, part of which reaches into the unexplored parameter space within the axion window. For the mass range from 3.2 to 24.3 μeV , we improve the previous constraint by a factor about $e^{1/2}$ within the axion window. The major improvement in the constraint comes from the QZE. In addition, our theoretical approach can also be utilized to search for other exotic spin-dependent interactions, such as those between the polarized electrons, and between a polarized electron and an unpolarized nucleon. Since it has not yet been implemented in the experiments, we do not only provide the optimal measurement parameters but also obtain optimal amplification, i.e., about 8900, and the corresponding time for the practical experiments, which can effectively guide related experiment in this work. We hope that the experiment could be realized in this overlapping spin ensemble by the QZE in the near future, contributing to the detection of exotic interactions and ALPs.

V. CONCLUSION

In this paper, we propose a noble-gas spin evolution in the dark and amplifying the measurement of the weak magnetic field by the QZE. Recently, there has been significant progress in amplifying the weak magnetic

field with mixtures of nuclear-spin-polarized noble gases and vapors of spin-polarized alkali-metal atoms, such as ^{129}Xe - ^{87}Rb [5, 26, 58]. The experimental process generally includes three necessary steps. First of all, we polarize alkali-metal spins with optical pumping and then noble-gas nuclear spins are polarized through spin-exchange collisions with polarized alkali-metal atoms spins. Secondly, the transverse magnetization generated by these nuclear spins produces effective fields on alkali-metal spins, which leads to magnetic amplification process. Finally, we measure the effective magnetic fields and calibrate the parameters of noble gases' spins with the magnetometer of alkali-metal atoms. In general, the dynamics of any open quantum system is initialized by a Gaussian decay [59], where the QZE occurs. It is followed by the Markovian dynamics and finalized by an power-law decay. However, the QZE is not restricted to the open quantum systems and can be generalized to closed quantum systems, which is an intrinsic effect due to the unitarity in quantum mechanics. As experimentally demonstrated in Ref. [42], the decoherence time T can be effectively prolonged by decreasing the pressure of the overlapping-spin ensemble. This technique can also be applied to various alkali-metal atoms and noble gases, including K - ^{129}Xe , K - ^3He and ^{87}Rb - ^{21}Ne , etc. In the experiments, the two main factors that affect the coherence time of the noble gas are the effective magnetic-field gradient from the polarization of alkali-metal atoms and the magnetic-field gradient from the applied field [26]. Therefore, decreasing the pressure of the overlapping-spin ensemble can not

affect coherence time of the noble gas. If the QZE is applied to this technique, this series of experiments will be enhanced with a more significant magnetic-field amplification effect. And thus it can be used to search for axions, dark photons and axion-mediated spin-dependent interactions, etc. Since the results of this work provide more significant magnetic amplification, we hope that our studies will stimulate experiments on establishing new constraints of dark matter and exotic interactions by this method.

In summary, we exploit the magnetic amplification considering the QZE through effective fields from collisions between alkali-metal atoms and noble-gas atoms, increasing the magnetic magnification by up to about 1.65-fold relative to the Markovian noise. Based on our analysis, we obtain the optimal time required to reach the maximum transverse polarization and thus the optimal response under different combinations of the parameters. Our results indicate that the amplification of measuring the weak fields can be further enhanced by the QZE as compared to the Markovian case. This indicates that our research can further improve the accuracy of weak field measurements.

ACKNOWLEDGMENTS

This work is supported by Innovation Program for Quantum Science and Technology under Grant No. 2023ZD0300200, the National Natural Science Foundation of China under Grant No. 62461160263, Beijing Natural Science Foundation under Grant No. 1202017, and Beijing Normal University under Grant No. 2022129.

-
- [1] D. N. Spergel, The dark side of cosmology: Dark matter and dark energy, *Science* **347**, 1100 (2015).
 - [2] G. Bertone and D. Hooper, History of dark matter, *Rev. Mod. Phys.* **90**, 045002 (2018).
 - [3] P. Sikivie, Invisible axion search methods, *Rev. Mod. Phys.* **93**, 015004 (2021).
 - [4] Y. M. Andreev, D. Banerjee, B. Banto Oberhauser, J. Bernhard, P. Bisio, V. E. Burtsev, A. Celentano, N. Charitonidis, A. G. Chumakov, D. Cooke, P. Crivelli, E. Depero, A. V. Dermenev, S. V. Donskov, R. R. Dusaev, T. Enik, V. N. Frolov, A. Gardikiotis, S. G. Gerassimov, S. N. Gninenko, M. Hösken, M. Jeckel, V. A. Kachanov, A. E. Karneyeu, G. Kekelidze, B. Ketzer, D. V. Kirpichnikov, M. M. Kirsanov, V. N. Kolosov, S. G. Kovalenko, V. A. Kramarenko, L. V. Kravchuk, N. V. Krasnikov, S. V. Kuleshov, V. E. Lyubovitskij, V. Lysan, L. Marsicano, V. A. Matveev, Y. V. Mikhailov, L. Molina Bueno, D. V. Peshekhonov, V. A. Polyakov, B. Radics, A. Rubbia, K. M. Salamatin, V. D. Samoylenko, H. Sieber, D. Shchukin, O. Soto, V. O. Tikhomirov, I. V. Tlisova, A. N. Toropin, B. I. Vasilishin, P. V. Volkov, V. Y. Volkov, I. Voronchikhin, and J. Zamora-Saá (NA64 Collaboration), Search for a new B - L Z' gauge boson with the NA64 experiment at CERN, *Phys. Rev. Lett.* **129**, 161801 (2022).
 - [5] H. Su, Y. Wang, M. Jiang, W. Ji, P. Fadeev, D. Hu, X. Peng, and D. Budker, Search for exotic spin-dependent interactions with a spin-based amplifier, *Sci. Adv.* **7**, eabi9535 (2021).
 - [6] Y. Hochberg, I. Charaev, S.-W. Nam, V. Verma, M. Colangelo, and K. K. Berggren, Detecting sub-GeV dark matter with superconducting nanowires, *Phys. Rev. Lett.* **123**, 151802 (2019).
 - [7] J. Manley, M. D. Chowdhury, D. Grin, S. Singh, and D. J. Wilson, Searching for vector dark matter with an optomechanical accelerometer, *Phys. Rev. Lett.* **126**, 061301 (2021).
 - [8] D. DeMille, J. M. Doyle, and A. O. Sushkov, Probing the frontiers of particle physics with tabletop-scale experiments, *Science* **357**, 990 (2017).
 - [9] M. S. Safronova, D. Budker, D. DeMille, D. F. J. Kimball, A. Derevianko, and C. W. Clark, Search for new physics with atoms and molecules, *Rev. Mod. Phys.* **90**, 025008 (2018).
 - [10] R. Bradley, J. Clarke, D. Kinion, L. J. Rosenberg, K. van Bibber, S. Matsuki, M. Mück, and P. Sikivie, Microwave cavity searches for dark-matter axions, *Rev. Mod. Phys.* **75**, 777 (2003).
 - [11] V. Anastassopoulos, S. Aune, K. Barth, A. Belov, H. Bräuninger, G. Cantatore, J. M. Carmona, J. F.

- Castel, S. A. Cetin, F. Christensen, J. I. Collar, T. Dafni, M. Davenport, T. A. Decker, A. Dermenev, K. Desch, C. Eleftheriadis, G. Fanourakis, E. Ferrer-Ribas, H. Fischer, J. A. García, A. Gardikiotis, J. G. Garza, E. N. Gazis, T. Gerasis, I. Giomataris, S. Gninenko, C. J. Hailey, M. D. Hasinoff, D. H. H. Hoffmann, F. J. Iguaz, I. G. Irastorza, A. Jakobsen, J. Jacoby, K. Jakovčić, J. Kaminski, M. Karuza, N. Kralj, M. Krčmar, S. Kostoglou, C. Krieger, B. Lakić, J. M. Laurent, A. Liolios, A. Ljubičić, G. Luzón, M. Maroudas, L. Miceli, S. Neff, I. Ortega, T. Papaevangelou, K. Paraschou, M. J. Pivovarov, G. Raffelt, M. Rosu, J. Ruz, E. R. Chóliz, I. Savvidis, S. Schmidt, Y. K. Semertzidis, S. K. Solanki, L. Stewart, T. Vafeiadis, J. K. Vogel, S. C. Yildiz, K. Zioutas, and C. A. S. T. Collaboration, New cast limit on the axion-photon interaction, *Nat. Phys.* **13**, 584 (2017).
- [12] T. Braine, R. Cervantes, N. Crisosto, N. Du, S. Kimes, L. J. Rosenberg, G. Rybka, J. Yang, D. Bowring, A. S. Chou, R. Khatiwada, A. Sonnenschein, W. Wester, G. Carosi, N. Woollett, L. D. Duffy, R. Bradley, C. Boutan, M. Jones, B. H. LaRoque, N. S. Oblath, M. S. Taubman, J. Clarke, A. Dove, A. Eddins, S. R. O’Kelley, S. Nawaz, I. Siddiqi, N. Stevenson, A. Agrawal, A. V. Dixit, J. R. Gleason, S. Jois, P. Sikivie, J. A. Solomon, N. S. Sullivan, D. B. Tanner, E. Lentz, E. J. Daw, J. H. Buckley, P. M. Harrington, E. A. Henriksen, and K. W. Murch (ADMX Collaboration), Extended search for the invisible axion with the axion dark matter experiment, *Phys. Rev. Lett.* **124**, 101303 (2020).
- [13] J. L. Ouellet, C. P. Salemi, J. W. Foster, R. Henning, Z. Bogorad, J. M. Conrad, J. A. Formaggio, Y. Kahn, J. Minervini, A. Radovinsky, N. L. Rodd, B. R. Safdi, J. Thaler, D. Winklehner, and L. Winslow, First results from abracadabra-10 cm: A search for sub- μeV axion dark matter, *Phys. Rev. Lett.* **122**, 121802 (2019).
- [14] M. Jiang, H. Su, Z. Wu, X. Peng, and D. Budker, Floquet maser, *Sci. Adv.* **7**, eabe0719 (2021).
- [15] S. Kotler, N. Akerman, Y. Glickman, A. Keselman, and R. Ozeri, Single-ion quantum lock-in amplifier, *Nature* **473**, 61 (2011).
- [16] S. C. Burd, R. Srinivas, J. J. Bollinger, A. C. Wilson, D. J. Wineland, D. Leibfried, D. H. Slichter, and D. T. C. Allcock, Quantum amplification of mechanical oscillator motion, *Science* **364**, 1163 (2019).
- [17] M. Jiang, Y. Qin, X. Wang, Y. Wang, H. Su, X. Peng, and D. Budker, Floquet spin amplification, *Phys. Rev. Lett.* **128**, 233201 (2022).
- [18] M. Schaffry, E. M. Gauger, J. J. L. Morton, and S. C. Benjamin, Proposed spin amplification for magnetic sensors employing crystal defects, *Phys. Rev. Lett.* **107**, 207210 (2011).
- [19] A. Zavatta, J. Fiurásek, and M. Bellini, A high-fidelity noiseless amplifier for quantum light states, *Nat. Photonics* **5**, 52 (2011).
- [20] S. Afach, B. Buchler, D. Budker, C. Dailey, A. Derevianko, V. Dumont, N. Figueroa, I. Gerhardt, Z. Grujić, H. Guo, C. Hao, P. Hamilton, M. Hedges, D. Jackson K., D. Kim, S. Khamis, T. Kornack, V. Lebedev, Z.-T. Lu, H. Masia-Roig, M. Monroy, M. Padniuk, C. Palm, S. Park, K. Paul, A. Penafior, X. Peng, M. Pospelov, R. Preston, S. Pustelny, T. Scholtes, P. Segura, Y. Semertzidis, D. Sheng, Y. Shin, J. Smiga, J. Stalnaker, I. Sulai, D. Tandon, T. Wang, A. Weis, A. Wickenbrock, T. Wilson, T. Wu, D. Wurm, W. Xiao, Y. Yang, D. Yu, and J. Zhang, Search for topological defect dark matter with a global network of optical magnetometers, *Nat. Phys.* **17**, 1396 (2021).
- [21] C. Dailey, C. Bradley, J. D. Kimball, I. Sulai, S. Pustelny, A. Wickenbrock, and A. Derevianko, Quantum sensor networks as exotic field telescopes for multi-messenger astronomy, *Nat. Astron.* **5**, 150 (2021).
- [22] J. Chang, R. Essig, and S. McDermott, Supernova 1987A constraints on sub-GeV dark sectors, millicharged particles, the QCD axion, and an axion-like particle, *J. High Energy Phys.* **2018** (9), 51.
- [23] A. Almasi, J. Lee, H. Winarto, M. Smiciklas, and M. Romalis, New limits on anomalous spin-spin interactions, *Phys. Rev. Lett.* **125**, 201802 (2020).
- [24] J. Lee, A. Almasi, and M. Romalis, Improved limits on spin-mass interactions, *Phys. Rev. Lett.* **120**, 161801 (2018).
- [25] G. Vasilakis, J. M. Brown, T. W. Kornack, and M. V. Romalis, Limits on new long range nuclear spin-dependent forces set with a $\text{K-}^3\text{He}$ comagnetometer, *Phys. Rev. Lett.* **103**, 261801 (2009).
- [26] M. Jiang, Y. Huang, C. Guo, H. Su, Y. Wang, X. Peng, and D. Budker, Observation of magnetic amplification using dark spins, *Proc. Natl. Acad. Sci. U. S. A.* **121**, e2315696121 (2024).
- [27] B. Misra and E. C. G. Sudarshan, The Zeno’s paradox in quantum theory, *J. Math. Phys.* **18**, 756 (1977).
- [28] A. Peres and A. Ron, Incomplete “collapse” and partial quantum Zeno effect, *Phys. Rev. A* **42**, 5720 (1990).
- [29] E. Block and P. R. Berman, Quantum Zeno effect and quantum Zeno paradox in atomic physics, *Phys. Rev. A* **44**, 1466 (1991).
- [30] Q. Ai, Y. Li, H. Zheng, and C. P. Sun, Quantum anti-Zeno effect without rotating wave approximation, *Phys. Rev. A* **81**, 042116 (2010).
- [31] D. Z. Xu, Q. Ai, and C. P. Sun, Dispersive-coupling-based quantum Zeno effect in a cavity-QED system, *Phys. Rev. A* **83**, 022107 (2011).
- [32] P. Facchi and S. Pascazio, Quantum Zeno dynamics: Mathematical and physical aspects, *J. Phys. A: Math. Theor.* **41**, 493001 (2008).
- [33] L.-A. Wu, D. A. Lidar, and S. Schneider, Long-range entanglement generation via frequent measurements, *Phys. Rev. A* **70**, 032322 (2004).
- [34] A. W. Chin, S. F. Huelga, and M. B. Plenio, Quantum metrology in non-Markovian environments, *Phys. Rev. Lett.* **109**, 233601 (2012).
- [35] Y. Matsuzaki, S. C. Benjamin, and J. Fitzsimons, Magnetic field sensing beyond the standard quantum limit under the effect of decoherence, *Phys. Rev. A* **84**, 012103 (2011).
- [36] X. Long, W.-T. He, N.-N. Zhang, K. Tang, Z. Lin, H. Liu, X. Nie, G. Feng, J. Li, T. Xin, Q. Ai, and D. Lu, Entanglement-enhanced quantum metrology in colored noise by quantum Zeno effect, *Phys. Rev. Lett.* **129**, 070502 (2022).
- [37] W. Itano, D. J. Heinzen, J. J. Bollinger, and D. J. Wineland, Quantum Zeno effect, *Phys. Rev. A* **41**, 2295 (1990).
- [38] C. Balzer, R. Huesmann, W. Neuhauser, and P. Toschek, The quantum Zeno effect-evolution of an atom impeded by measurement, *Opt. Commun.* **180**, 115 (2000).
- [39] M. C. Fischer, B. Gutiérrez-Medina, and M. G. Raizen,

- Observation of the quantum Zeno and anti-Zeno effects in an unstable system, *Phys. Rev. Lett.* **87**, 040402 (2001).
- [40] S. Wilkinson, C. Bharucha, M. Fischer, K. Madison, P. Morrow, Q. Niu, B. Sundaram, and M. Raizen, Experimental evidence for non-exponential decay in quantum tunnelling, *Nature* **387**, 575 (1997).
- [41] E. Streed, J. Mun, M. Boyd, G. Campbell, P. Medley, W. Ketterle, and D. Pritchard, Continuous and pulsed quantum Zeno effect, *Phys. Rev. Lett.* **97**, 260402 (2006).
- [42] B. Nagels, L. J. F. Hermans, and P. L. Chapovsky, Quantum Zeno effect induced by collisions, *Phys. Rev. Lett.* **79**, 3097 (1997).
- [43] F. Schäfer, I. Herrera, S. Cherukattil, C. Lovecchio, F. S. Cataliotti, F. Caruso, and A. Smerzi, Experimental realization of quantum Zeno dynamics, *Nat. Commun.* **5**, 3194 (2014).
- [44] N. Kalb, J. Cramer, D. J. Twitchen, M. Markham, R. Hanson, and T. H. Taminiau, Experimental creation of quantum Zeno subspaces by repeated multi-spin projections in diamond, *Nat. Commun.* **7**, 13111 (2016).
- [45] A. Potočnik, A. Bargerbos, F. A. Y. N. Schröder, S. A. Khan, M. C. Collodo, S. Gasparinetti, Y. Salathé, C. Creatore, C. Eichler, H. E. Türeci, A. W. Chin, and A. Wallraff, Studying light-harvesting models with superconducting circuits, *Nat. Commun.* **9**, 904 (2018).
- [46] K. Kakuyanagi, T. Baba, Y. Matsuzaki, H. Nakano, S. Saito, and K. Semba, Observation of quantum Zeno effect in a superconducting flux qubit, *New J. Phys.* **17**, 063035 (2015).
- [47] D. H. Slichter, C. Müller, R. Vijay, S. J. Weber, A. Blais, and I. Siddiqi, Quantum Zeno effect in the strong measurement regime of circuit quantum electrodynamics, *New J. Phys.* **18**, 053031 (2016).
- [48] L. Bretheau, P. Campagne-Ibarcq, E. Flurin, F. Mallet, and B. Huard, Quantum dynamics of an electromagnetic mode that cannot contain N photons, *Science* **348**, 776 (2015).
- [49] H. Su, M. Jiang, Y. Wang, Y. Huang, X. Kang, W. Ji, X. Peng, and D. Budker, New constraints on axion-mediated spin interactions using magnetic amplification, *Phys. Rev. Lett.* **133**, 191801 (2024).
- [50] M. H. Levitt, *Spin Dynamics: Basics of Nuclear Magnetic Resonance*, 2nd ed. (John Wiley & Sons, UK, 2013).
- [51] H. P. Breuer and F. Petruccione, *The Theory of Open Quantum Systems* (Oxford University Press, New York, 2002).
- [52] T. Walker and W. Happer, Spin-exchange optical pumping of noble-gas nuclei, *Rev. Mod. Phys.* **69**, 629 (1997).
- [53] N. F. Ramsey, The tensor force between two protons at long range, *Physica (Amsterdam)* **96A**, 285 (1979).
- [54] A. G. Glenday, C. E. Cramer, D. F. Phillips, and R. L. Walsworth, Limits on anomalous spin-spin couplings between neutrons, *Phys. Rev. Lett.* **101**, 261801 (2008).
- [55] J. E. Moody and F. Wilczek, New macroscopic forces?, *Phys. Rev. D* **30**, 130 (1984).
- [56] B. A. Dobrescu and I. Mocioiu, Spin-dependent macroscopic forces from new particle exchange, *J. High Energy Phys.* **2006** (11), 005.
- [57] P. Fadeev, Y. V. Stadnik, F. Ficek, M. G. Kozlov, V. V. Flambaum, and D. Budker, Revisiting spin-dependent forces mediated by new bosons: Potentials in the coordinate-space representation for macroscopic- and atomic-scale experiments, *Phys. Rev. A* **99**, 022113 (2019).
- [58] M. Jiang, H. Su, A. Garcon, X. Peng, and D. Budker, Search for axion-like dark matter with spin-based amplifiers, *Nat. Phys.* **17**, 1402 (2021).
- [59] H. Nakazato, M. Namiki, and S. Pascazio, Temporal behavior of quantum mechanical systems, *Int. J. Mod. Phys. B* **10**, 247 (1996).